Predicting Scour at Bridge Piers

Jean-Louis Briaud

Spencer J. Buchanan Professor, Department of Civil Engineering, Texas A&M University, College Station

ABSTRACT

A new method called SRICOS is proposed to predict the scour depth z versus time t around a cylindrical bridge pier of diameter D founded in clay. The steps involved are: 1. taking samples at the bridge pier site, 2. testing them in an Erosion Function Apparatus called the EFA to obtain the scour rate z versus the hydraulic shear stress applied τ, 3. predicting the maximum shear stress τ max which will be induced around the pier by the water flowing at ν 0 before the scour hole starts to develop, 4. using the measured z versus τ curve to obtain the initial scour rate *zi* corresponding to τ max , 5. predicting the maximum depth of scour *zmax* for the pier, 6. using *zi* and *zmax* to develop the hyperbolic function describing the scour depth z versus time t curve, and 7. reading the z vs. t curve at a time corresponding to the duration of the flood to find the scour depth which will develop around the pier.

A new apparatus is developed to measure the z vs t curve of step 2, a series of advanced numerical simulations are performed to develop an equation for the τ max value of step 3, and a series of flume tests are performed to develop an equation for the *zmax* value of step 5. The method is evaluated by comparing predictions and measurements in 42 flume experiments.

INTRODUCTION

There are approximately 600,000 bridges in the United States and 500,000 of them are over water (National Bridge Inventory, 1997). During the last 30 years over 1000 of the 600,000 bridges have failed and 60% of those failures are due to scour with earthquake accounting for only 2% (Shirole and Holt, 1991). The average cost for flood damage repair of highways on the Federal aid system is 50 million dollars per year (Lagasse et al., 1995).

On April 5, 1987 a 32 year old bridge over Schoharie Creek in the State of New York collapsed when the spread footing foundation became undermined by pier scour. This collapse

and the associated deaths prompted the Federal Highway Administration to ask the State Departments of Transportation for an evaluation of their over-water bridges for scour susceptibility. The result of this 10 year effort shows that 62.4% of these bridges have a low risk of scour failure, 13.5% are scour susceptible, 20.0% have unknown foundations, 0.6% is left to be screened and 3.5% or about 17,000 bridges are scour critical which means that they are likely to fail if they are subjected to a 100 year flood (Pagan-Ortiz, 1998). These numbers indicate the importance of the bridge scour problem.

Research on bridge scour has been active since at least the late fifties. The Schoharie bridge failure prompted an increase in sponsored research with about 11 million dollars spent over the last 6 years (Parola, 1997). Most of this research has been dedicated to bridge scour in sand the topic of this article is bridge scour in clay , more specifically the prediction of the scour depth vs time curve for circular piers founded in clay. Does clay scour to the same final depth of scour as sand? How fast does clay scour? These are some of the questions addressed.

CURRENT PRACTICE

Scour can be divided into general scour (general erosion of the stream bed without obstacles), local scour (scour generated by the presence of obstacles such as piers and abutments, Fig. 1), and channel migration (lateral movement of the main stream channel). Current practice is heavily influenced by two FHWA hydraulic engineering circulars called HEC-18 and HEC-20 (Richardson and Davis, 1995; Lagasse et al., 1995). For pier scour, the topic of this study, HEC-18 recommends the use of the following equation to predict the maximum depth of scour z_{max} above which all soil resistance must be discounted:

$$z_{max} = 2 z_o K_1 K_2 K_3 K_4 \left(\frac{D}{z_o}\right)^{0.65} F_o^{0.43} \quad (1)$$

where z_o is the depth of flow just upstream of the bridge pier excluding local scour, K_1, K_2, K_3, K_4 are coefficients to take into account the shape of the pier, the angle between the direction of the flow and the direction of the pier, the stream bed topography, and the armoring effect, D is the pier diameter, and F_o is the Froude number defined as $v/(gz_o)^{0.5}$ where v is the mean flow velocity and g is the acceleration due to gravity.

This equation is based on model scale experiments in sand and has recently been evaluated (Fig. 2) against full scale observations for 56 bridges founded primarily on sand (Landers and Mueller, 1996). Nothing in HEC-18 gives guidance to calculate the rate of scour in clay and it is implicit that (1) should also be used for the final depth of scour for bridges on clay. Common sense tells us that clays scour much more slowly than sand and using (1) for clays regardless of time appears to be overly conservative and therefore expensive. The potential savings in this respect is what prompted sponsorship of this research.

SHEAR STRESS IMPOSED

The scour process is highly dependant on the shear stress developed by the flowing water at the soil-water interface. Indeed, at that interface the flow is tangential to the soil surface regardless of the flow condition above it; very little water if any flows perpendicular to the interface. The water velocity in the river is in the range of 0.1 m/s to 3 m/s while the bed shear stress is in the range of 1 to 50 N/m^2 and increases with the square of the water velocity. The magnitude of this shear stress is a very small fraction of the undrained shear strength of clays used in foundation engineering for example (Fig. 3). It is amazing to see that such small shear stresses are able to scour rocks to a depth of 1600 m as is the case for the Grand Canyon over the last 20 million years at an average scour rate of 9×10^{-6} mm/hr. This leads one to think that even small shear stresses if applied cyclically by the turbulent nature of the flow can overcome, after a

sufficient number of cycles, the crystalline bonds in a rock and the electromagnetic bonds in a clay. This also leads one to think that there is no cyclic stress threshold but that any stress is associated with a number of cycles to failure. Gravity bonds seem to be an exception to this postulate as it appears that gravity bonds cannot be weakened by cyclic loading. This postulate contradicts the critical shear stress concept discussed later.

The shear stress τ imposed by the water at a boundary can be evaluated in a number of ways. The first one is for open channels without obstructions and is based on equilibrium considerations (Munson et al., 1990):

$$\tau = r_h S_{EGL} \gamma_w \tag{2}$$

where r_h is the hydraulic radius defined as the cross section area of the flow divided by the wetted perimeter, S_{EGL} the slope of the Energy Grade Line (slope of the river bed generally), and γ_w the unit weight of water. The second one is for circular pipes without obstructions and is also based on equilibrium considerations (Munson et al., 1990):

$$\tau = \frac{R}{2} \times \Delta p/\ell \tag{3}$$

where R is the pipe radius and $\Delta p/\ell$ is the pressure drop Δp per length ℓ of pipe. The pressure drop can either be measured or calculated by using the Moody Chart (Munson et al, 1990, p. 501).

When a cylinder obstructs the flow in an open channel with a flat bottom, the maximum shear stress τ_{max} is located as shown on Fig. 4 and is many times larger than the value given when there is no obstructions (2). In this study a detailed numerical simulation, described later, was performed (Wei et al., 1997) to obtain τ_{max}. It was found (Fig. 5) that, for large water depth ($Z_o/D > 2$), τ_{max} was dependent on the Reynold's number R_e, the mean flow velocity

V and the mass density of water ρ :

$$\tau_{max} = 0.094\,\rho\,V^2\left(\frac{1}{\log R_e} - \frac{1}{10}\right) \quad (4)$$

where the Reynold's number R_e is defined as VD/ν where V is the mean flow velocity, D is the pier diameter, and ν is the kinematic viscosity of water (10^{-6} m^2/s at 20° C). If this value of τ_{max} is larger than the critical shear stress τ_c that the soil can resist, scour is initiated. As the scour hole deepens around the cylinder the shear stress at the bottom of the hole decreases. A profile of the shear stress at the bottom of the scour hole τ_{bot} as a function of the depth of the scour hole, using the same numerical analysis, is shown in Fig. 6. Once the scour hole becomes deep enough, τ_{bot} becomes equal to τ_c (the critical shear stress for the soil), the soil stops scouring, and the final depth of scour z_{max} is reached.

CRITICAL SHEAR STRESS

The critical shear stress τ_c is the shear stress imposed by the water on the soil when scour is initiated. Below this shear stress the soil particles are not displaced, above this shear stress the soil particles are transported away and a certain scour rate is established. As discussed earlier this concept may not be theoretically correct however it is practically useful. It may be that a more acceptable definition of τ_c is the shear stress corresponding to a standardized small erosion rate. For the experiments in this study, this threshold erosion rate was taken as 1 mm/hr (EFA) as an arbitrary limit which would create only 168 mm of scour for a week-long flood.

In the case of sand and gravel, the scour process is controlled by the weight of the particles and one way to estimate τ_c is to calculate the shear force T necessary for the water to overcome the friction between two stacked particles:

$$T = W \tan \phi = (\rho_s - \rho_w)\, g \frac{\pi d^3}{6} \tan \phi \qquad (5)$$

where W is the weight of the particle, ϕ the friction angle, ρ_s and ρ_w the mass density of the sand particle and water respectively, g the acceleration due to gravity, and d the diameter of the sand particle which is assumed to be spherical. The drag force F applied by the water on the particle is

$$F = \tau A_e \qquad (6)$$

where A_e is the effective area of the sand particle over which the hydraulic shear stress τ is applied. If A_e is expressed as a fraction α of the particle maximum cross section ($\pi \frac{d^2}{4}$), the expression for τ_c comes from equating (5) and (6).

$$\tau_c = \frac{2 (\rho_s - \rho_w)\, g d \tan \phi}{3 \alpha} \qquad (7)$$

Experiments were performed to evaluate the coefficient α . A uniform sand and a uniform gravel were tested in the Erosion Function Apparatus developed for this research and described later. Table 1 shows the results obtained: The values of α in Table 1 were obtained by assuming the following values of the other parameters in (7): $\rho_s = 2650\ kg/m^3$, $\rho_w = 1000\ kg/m^3$, $g = 9.81\ m/s^2$, $d = d_{50}$, $\phi = 30°$. The mean α value was 6.14.

The value of α is surprisingly high because one would expect α to be less than one. This shows that the assumed scour process by sliding is at best incomplete. Close observations on slow motion videotapes show that the scour process is a combination of rolling, sliding and plucking of the particle. It also shows that the turbulence in the water at the soil-water interface induces cyclic loading on the particles.

The average ratio between the measured values of τ_c in N/m^2 and d_{50} in mm is 1.03 and

leads to the equation

$$\tau_c\,(N/m^2) = d_{50}\,(mm) \qquad \textbf{(8)}$$

while the data is very limited (Table 1), the equation proposed by Laursen (1962) is similar to equation (8) and consistent with earlier data by Shields:

$$\tau_c\,(N/m^2) = 0.63\,d_{50}\,(mm) \qquad \textbf{(9)}$$

In the case of silts and clays, other forces come into play besides the weight of the particles; these are the electrostatic and Van der Waals forces. Electrostatic forces are likely to be repulsive because clay particles are negatively charged. Van der Waals forces are relatively weak electromagnetic forces which attract molecules to each other (Mitchell, 1993); although electrically neutral, the molecules form dipoles which attract each other like magnets. The Van der Waals forces are the forces which keep H_2O molecules together in water. The magnitude of these Van der Waals forces can be estimated by (after Black et al., 1960):

$$f(N/m^2) = \frac{10^{-28}}{d\,(m)^4} \qquad \textbf{(10)}$$

where *d(m)* is the distance in *m* between soil particles, and *f* is the attraction force in N/m^2. By multiplying *f* by the particle surface area, one can obtain the interparticle force. Table 2 shows the value of these forces for a sand and a clay particle. In both cases the soil particle was assumed to be spherical and the distance between particles was taken equal to the particle diameter. While such an evaluation of the Van der Waals force can only be considered as a crude estimate, the following observations regarding the numbers in Table 2 are interesting. First, the ratio between the weight of the sand particle and of the clay particle is similar to the ratio between

the weight of a Boeing 747 and of a postage stamp; therefore if the critical shear stress is proportional to the particle weight, the critical shear stress for clays is practically zero. Second, the ratio between the Van der Waals force and the weight of the sand particle indicates that the Van der Waals force is truly negligible for sands. Third, the same ratio for the clay particle, while many times larger than for sand, also indicates that the Van der Waals forces are negligible compared to the weight of the clay particle. This would lead one to think that the critical shear stress τ_c is essentially zero for clays. Note that the electrostatic forces have not been calculated here but since they are predominantly repulsive they would decrease, if anything, the attraction due to the Van der Waals forces. Other phenomena give cohesion to clays; they include water meniscus forces such as those developing when a clay dries, and diagenetic bonds due to aging such as those developing when a clay turns into rock under pressure and over geologic time. Because of the number and complexity of these bonds, it is very difficult to predict τ_c for clays empirically on the basis of a few index properties. Several researchers however have proposed empirical equations for τ_c in clays such as Dunn (1959) and Lyle and Smerdon (1965). In the approach described in this paper, it is preferred to measure τ_c directly for each clay in the new EFA test as described later.

One problem associated with measuring τ_c is determining the initiation of scour. When the particles are visible with the naked eyes, it is simple to detect when the first particle is scoured away. For clays this is not the case and various investigators define the initiation of scour through different means; these vary from "when the water becomes muddy" to extrapolation of the scour rate versus shear stress curve back to zero scour rate. Table 3 shows a wide variety of measured τ_c ; the lack of precise definition for the initiation of scour may be in part responsible for the wide range of values.

SCOUR RATE

Beyond the critical shear stress, a certain scour rate $\dot{z}$ (mm/hr) is established. This scour rate is rapid in sand, slow in clay and extremely slow in rocks. The example of the Grand Canyon rocks cited earlier leads to a value of $\dot{z}$ equal to 9×10^{-6} mm/hr while fine sands erode at rates of 10^4 mm/hr as measured in the EFA. Clays scour at intermediate rates with common values in the range of 1 to 1000 mm/hr (Table 4).

The high scour rate in sand exists because once gravity is overcome, no other force slows the scour process down. The very low scour rate in rock exists probably because it takes a large number of shear stress cycles imposed by the turbulent nature of the flow to overcome the very strong crystalline bonds binding the rock together. The low scour rate in clays is probably also associated with the fact that it takes a large number of shear stress cycles to overcome the electromagnetic bonds created by the Van der Waals forces between clay particles. Even though these bonds are relatively weak, as discussed previously, they are sufficient to slow the scour process significantly.

The scour rate $\dot{z}$ versus shear stress τ curve (Fig. 7) is used to quantify the scour rate of a soil as a function of the flow velocity in a stream. Several researchers have measured the rate of erosion in cohesive soils; most have proposed a straight line variation (DE on Fig.7) (Ariathurai, Arulanandan, 1978) while some have found S shape curves (OABC on Fig. 7) (Christensen, 1965). This S shape would indicate that different physical phenomena take place as the water velocity increases (Fig. 7).

THE SRICOS METHOD

SRICOS stands for Scour Rate In COhesive Soils; it is a method to predict the scour depth versus time curve around a cylindrical bridge pier standing in the way of a constant velocity flow

and founded in a uniform cohesive soil. The method consists of the following steps which are explained in the next sections. It is important for any engineer to understand the limitation of this proposed method before using it. These limitations are discussed later.

1. Obtain standard 76.2 mm diameter Shelby tube samples as close to the pier as possible.
2. Perform EFA (Erosion Function Apparatus) tests on the samples from the site to obtain the curve linking the erosion rate $\dot{z}$ and the hydraulic shear stress imposed τ .
3. Determine the maximum shear stress τ_{max} which will exist on the river bottom around the pier at the beginning of the scour process.
4. Obtain the initial scour rate $\dot{z}_i$ corresponding to τ_{max}.
5. Calculate the maximum depth of scour z_{max} .
6. Develop the complete scour depth z versus time t .
7. Predict the depth of scour by reading the z versus t curve at the time corresponding to the duration of the flood.

OBTAIN SAMPLES AND PERFORM EFA TESTS

SRICOS is a site specific scour prediction method because samples from the bridge site are collected and tested. The samples should be 76.2 mm diameter Shelby tube samples (ASTM-D1587) obtained close to the bridge pier. The samples are brought back to the laboratory where they are tested in the Erosion Function Apparatus (EFA).

The EFA (Figs. 8 and 9) is an apparatus which was developed for this study. The sample is pushed out of the Shelby tube by a piston only as fast as it takes to erode the soil by water flowing over it. The sample is pushed vertically upward into a test section which is made of a pipe with a rectangular cross-section; the Plexiglas pipe is 50.8 mm high and 101.6 mm wide to accommodate the 76.2 mm diameter sample. In a standard test, the sample is pushed so that it

protrudes 1 mm into the test section. The protrusion distance was varied from 0.1 mm to 2 mm. There was little difference between a protrusion of 0.1 mm, 0.5 mm and 1 mm. The 2 mm protrusion led to a higher scour rate; the protrusion distance was standardized to 1 mm. The water flows over the sample at a chosen velocity v and the sample is advanced another 1 mm as soon as it is eroded back to be flush with the bottom of the Plexiglas test section. This process is repeated for at least 1 hr and leads to an average erosion rate $\dot{z}$ for the velocity v. An electronic eye system was used at first to automate this process but the unevenness of the scoured sample surface often due to soil heterogeneity would create some erroneous scour rate readings. Pressure ports just before and just after the sample location give the differential pressure Δp necessary to calculate the shear stress τ applied by the water (3). The detail of these calculations is in (Perugu et al., 1999).

One test leads to one $\dot{z}$ and one corresponding τ value. Several tests are performed for a range of velocities varying between 0.1 m/s to 6 m/s. The corresponding range of τ values is approximately 0.1 N/m^2 to 100 N/m^2. A series of points ($\dot{z}$, τ) are obtained for the soil. A typical result on a porcelain clay is shown in Fig. 10. For comparison purposes, the $\dot{z}$ *vs* τ curve for a sand is also shown on Fig. 10. The properties of the clay are shown in Table 5. The $\dot{z}$ versus τ curve is not linear as often found in the literature but has a shape more similar to the results presented by Christensen (1965). In the EFA test it was considered that $\dot{z}$ was zero if $\dot{z}$ was less than 1 mm/hr. Therefore, the critical shear stress τ_c was defined as the shear stress which would generate a scour rate of 1 mm/hr (24 mm/day). This arbitrary number was used because in a week long flood event the scour depth would still be very small for 1 mm/hr.

MAXIMUM SHEAR STRESS AND INITIAL SCOUR RATE

In order to evaluate the maximum shear stress occurring around a cylindrical pier a numerical

simulation of the water flow was performed (Wei et al., 1997). The CHIMERA - RANS method was used (Chen, et al., 1996). Chimera is a dragon with the head of a lion, the body of a goat and the tail of a snake. This word is used to illustrate the fact that the total mesh representing the water is divided into several blocks of three dimensional elements later assembled to make a whole; this division is necessary to make the problem more mathematically manageable considering the very large number of elements involved. These often very different blocks of elements are assembled by mass and momentum conservation laws at the boundaries reminding one of the Chimera dragon. RANS stands for Reynolds-Averaged Navier Stokes equations. The Navier-Stokes equations and the continuity equation are four partial differential equations where the unknowns are the flow velocities (u, v, w) and the pressure p to be solved as a function of the position and time coordinates x, y, z, and t. These equations come from three equations of motion linking the stresses, one continuity equation linking the velocities, and six constitutive equations linking the stresses to the velocities by using the fact that water is a linear Newtonian viscous fluid. In laminar steady state flow u, v, w and p do not fluctuate at a given point and the Navier-Stokes equations plus the continuity equation are sufficient to solve the complete problem.

In turbulent steady state flow u, v, and w fluctuate (Fig. 11) around mean values in a random cyclic fashion; this is where the term Reynold's average comes from. The mean cyclic amplitude of the velocity fluctuations $\sqrt{\overline{u'^2}}$ divided by the mean velocity $\bar{u}$ is the turbulence intensity of the water flow with typical values for pier scour between 0.1 and 0.2. The mean frequency of the cycles can vary drastically and is likely in the 10 to 100 Hz range for pier scour. In modeling the turbulent flow, the equations of motion and the continuity equation remain the same but the mean amplitude of the velocity fluctuations introduces additional variables which

require additional modeling equations. The energy level in the water flow is used to characterize these additional velocity components; the layer eddy viscosity model is one of the models used to describe these additional velocity components (Chen, Patel, 1988).

One of the output of the computer simulation is the shear stress variation on the river bed around the pier (Fig. 4). This figure corresponds to the first step in the CHIMERA-RANS solution: the one for to a flat river bottom. A series of analyses of this flat river bottom or initial condition case were performed by varying the water velocity and the pier diameter. The results were used to prepare Fig. 5 and the associated (4) which gives the maximum shear stress τ_{max} around the pier for a flat river bottom condition. If τ_{max} is larger than the critical shear stress for the soil τ_c, scour will be initiated in regions where $\tau > \tau_c$. The initial scour rate $\dot{z}_i$ is then read on the $\dot{z}$ versus τ curve, obtained from the EFA tests on the soil sample, at the value of τ_{max}.

MAXIMUM DEPTH OF SCOUR

In order to evaluate the maximum depth of scour z_{max} for clay, a series of flume experiments were performed. The detailed description of those experiments can be found in Gudavalli et al. (1997). Two flumes were used; the first flume was 457 mm wide and the second 1525 mm wide. The diameter of the cylindrical piers varied from 25 mm to 76 mm for the smaller flume and from 76 mm to 229 mm for the larger flume. Four different soils were used: three clays and one sand. The water depth varied from 160 mm to 400 mm in the smaller flume and 250 mm to 400 mm in the larger flume while the velocity ranged from 0.204 m/s to 0.83 m/s in the smaller flume and 0.3 m/s to 0.404 m/s in the larger flume. A total of 42 experiments was performed. An example of the results obtained for each experiment is shown in Fig. 12 for a 75 mm diameter pier in the porcelain clay (Table 5).

Note on Fig. 12 that the scour hole is developing mostly behind the pier after starting near the location of τ_{max} on Fig. 4. This is quite different from what has been observed for scour in sand where the hole develops all around the pier. Therefore it would be more desirable for piles in clay to place any monitoring instrument behind the pier than in front of the pier.

As can also be seen on Fig. 12, the experiments were carried out for several days in order to approach the final depth of scour z_{max}; however z_{max} was not reached. In order to get a better estimate of z_{max} several models were used to curve fit the experimental scour depths vs time curve. The best fitting model was a hyperbola with the following equation:

$$z = \frac{t}{\frac{1}{\dot{z}_i} + \frac{t}{z_{max}}} \tag{11}$$

where $\dot{z}_i$ is the initial slope of the z versus t curve and z_{max} is the ordinate of the asymptote. The parameter z_{max} represents the final depth of scour at $t = \infty$. The curve fitted hyperbola is shown on Fig. 12. The definition of z_{max} as the asymptotic value of the hyperbola can be argued with; however it has the advantage to be a consistent definition for all experiments. The real proof of the model will be achieved if the predictions match the observed behavior on full scale bridges over long periods of time. This is an ongoing process.

The z_{max} values for all the experiments were obtained and were plotted against various parameters. It was found (Fig. 13) that the most well behaved relationship was obtained when plotting z_{max} versus the pier Reynold's number R_e:

$$R_e = \frac{VD}{\upsilon} \tag{12}$$

where V is the mean flow velocity, D the pier diameter and υ the kinematic viscosity of the water

(10^{-6} m^2/s at 20°C). The proposed relationship is:

$$z_{max}(mm) = 0.18\, R_e^{0.635} \quad \textbf{(13)}$$

The simplicity of this relationship is most attractive. Shen at al. (1969) developed a very similar one. This relationship and Fig. 13 lead to the following observations. First, the maximum depth of scour in sand and in clay appears to be the same; this is confirmed by the fact that the HEC-18 equation developed from sand experiments fits this data on clay quite well. Second, the Reynolds number which characterizes the ratio of inertia force over viscous force was found to be a better indicator of z_{max} than the Froude number which characterizes the ratio of inertia force to gravity force; this seems logical since from the hydraulics point of view the viscous force has more to do with the hydraulic shear stress and therefore the scour problem than the gravity force. Third, the water depth was varied in the experiments but was found to have very little influence on the results; hence, it does not appear in (13). This is confirmed to some extent by the fact that the power exponent on the water depth in the HEC-18 equation is very low (0.135). Fourth, the most important factors are the mean flow velocity V and the pier diameter D . For most common full scale flood situations (D between 1 m and 3 m and V between 2 m/s and 4 m/s) the ratio z_{max}/D varies between 2 and 4.

SCOUR DEPTH VERSUS TIME CURVE AND PREDICTION

The hyperbolic model of (11) can be used since $\dot{z}_i$ and z_{max} are now known. The initial rate of scour $\dot{z}_i$ is obtained from the erosion curve $\dot{z}$ versus τ generated with the EFA on samples from the site; $\dot{z}_i$ is found on that curve at the maximum shear stress τ_{max} which will occur around the pier to initiate scour; τ_{max} is obtained from (4) which is based on numerical modeling results. The value of z_{max} is obtained from (13) which is based on flume tests results. Therefore SRICOS requires the knowledge of the mean flow velocity of the stream v , the diameter of the

pier D and the erosion curve $\dot{z}$ versus τ from the EFA.

With $\dot{z}_i$ and z_{max} the complete scour depth z versus time t curve (11) is generated for the bridge pier (Fig. 14). Then the duration t_{design} of the design flood event is evaluated and the anticipated depth of scour z_{design} is read on the z, t curve at t_{design}.

In order to evaluate the precision of SRICOS, one can compare z_{max} predicted with z_{max} measured (Fig. 15). The measured values of z_{max} on Fig. 15 come from the flume tests performed in this study while the predicted values come from equation (13). The scatter in Fig. 15 is reasonably small; however this comparison between predicted and measured values is not a true evaluation of the precision of the z_{max} equation (13) since that equation was generated by using the same data base. In that sense Fig. 15 is likely to represent the most favorable comparison.

Another way to evaluate SRICOS is to compare $\dot{z}_i$ predicted with $\dot{z}_i$ measured (Fig. 16). The measured values of $\dot{z}_i$ on Fig. 16 come from the flume tests; the predicted values come from equation (4) to get τ_{max} and then reading $\dot{z}_i$ on the EFA generated $\dot{z}$ *vs* τ curve at τ_{max}. There is more scatter for $\dot{z}_i$ than for z_{max} which confirms that predicting small deformations is more erratic than predicting large deformations. The scatter for $\dot{z}_i$ however is similar to the one on Fig. 2. The best fit regression through the origin of Fig. 16 gives:

$$\dot{z}_{im} = 1.05\, \dot{z}_{ip} \qquad \textbf{(14)}$$

EXAMPLE

A bridge pier is 2 m in diameter in a river which will experience a flood velocity of 2 m/s for a duration of 4 days. Shelby tube samples of the clay were recovered at the site, tested in the

EFA and lead to the scour rate $\dot{z}$ versus shear stress τ curve of Fig. 10b. The maximum shear stress τ_{max} around the pier before scour begins is given by (4).

$$\tau_{max} = 0.094 \times 1000 \times 2^2 \left(\frac{1}{\log \frac{2 \times 2}{10^{-6}}} - \frac{1}{10} \right) = 19.4 \frac{N}{m^2}$$

For this τ_{max} value, the initial rate of scour $\dot{z}_i$ is found on Fig. 10b:

$$\dot{z}_i = 8.5 \; mm/hr$$

The maximum depth of scour z_{max} is calculated according to (13)

$$z_{max}(mm) = 0.18 \times \left(\frac{2 \times 2}{10^{-6}} \right)^{0.635} = 2803 \; mm$$

Then the complete depth of scour z versus time t curve is generated according to (11) (Fig. 14):

$$z\,(mm) = \frac{t\,(hrs)}{\frac{1}{8.5} + \frac{t\,(hrs)}{2803}}$$

After 4 days or 96 hours, the scour depth z is

$$z\,(mm) = \frac{96}{\frac{1}{8.5} + \frac{96}{2803}} = 632 \; mm$$

In this case the scour depth is only 22.5% of the maximum scour depth.

FUTURE IMPROVEMENTS OF THE SRICOS METHOD

In the quest for continuous improvement one should at least demonstrate that any new method is better than all currently used methods. Since, at present, there is essentially no commonly used method to predict the scour depth versus time curve for a pier in clay, SRICOS represents an improvement corresponding to an initial step filling up a void. At the same time

SRICOS has limitations which need to be discussed so that the engineer can make more educated decisions.

The method needs to be compared with full scale scour measurements. The biggest pier that SRICOS has been evaluated against is 230 mm in diameter at a velocity of 0.4 m/s. Comparisons with a number of piers with diameters of the order of 2000 mm and velocities of about 3 m/s are desirable. Some confidence comes from the fact that the HEC-18 equation fits the z_{max} data well and that the HEC-18 equation has been checked at full scale.

SRICOS has been developed for the simplest case of a circular pier. Bridge piers with different shapes will likely lead to somewhat different scour depth versus time curves. In first approximation, one might use the shape correction factor proposed for sand in (1). For that matter the other coefficients in (1) which are for the difference in direction between the pier and the flow, for the stream bed topography, and for the armoring effect could also be used while waiting for the same data to be developed for clays.

The data indicate that the maximum depth of scour z_{max} may be the same for clay and for sand; this would imply that the scour hole stops becoming deeper at the same shear stress whether in clay or in sand. This would then imply that the critical shear stress τ_c is the same for sand and clay which is not what current data indicates. The premise that z_{max} is the same for sands and clays, and yet that τ_c is different for sands and clays is a puzzle which needs to be addressed.

The site specific aspect of SRICOS through sampling at the site is an advantage yet the volume of soil sampled represents a very small fraction of the volume to be scoured around the pier (e.g.: 0.05%). This will induce scatter because of the natural heterogeneity of the soil. One way to remedy this situation is to use geophysical methods which can give a complete scan of the area with depth at a reasonable cost and use the scan to extend the result obtained on the samples.

Two aspects of the EFA can be improved. First, the pressure in the test section is not controlled; it is whatever is generated by the water velocity. A valve on the downstream side of the test section can be used to run tests at different pressures but at the same velocity. This would indicate the influence of the water pressure or normal stress on the $\dot{z}$ versus τ curve. Second, the turbulence intensity in the test section is not controlled; it is whatever is generated by the water velocity and the roughness of the wall. Placing adjustable obstacles on the walls could be used to vary the turbulence intensity while measuring it qualitatively with the pressure versus time signal. This would indicate the influence of the turbulence intensity on the $\dot{z}$ versus τ curve.

ALTERNATIVE METHOD

The CHIMERA-RANS numerical simulation method can be used to predict the complete scour history in three dimensions (Wei et al., 1997). This is achieved by attaching a soil erosion model to the current CHIMERA-RANS hydraulic model. The procedure steps into time and at each time step the shear stresses τ at the water-soil interface are calculated, the scour rate $\dot{z}$ is determined at each location by reading the $\dot{z}$ versus τ curve at the proper τ. For the following time step, the water soil interface is lowered in the simulation mesh by an amount equal to $\dot{z}\Delta t$ at each location. With this new profile of the interface, CHIMERA-RANS predicts a new set of hydraulic shear stresses τ, which leads to a new set of soil scour rate values $\dot{z}$, which scours the river bottom by $\dot{z}\Delta t$, and the process goes on until τ becomes smaller or equal to the critical shear stress τ_c at all locations along the water-soil interface.

Such a process with the CHIMERA-RANS program will tie up an average work station for at least 24 hours. A comparison between predicted and measured results is shown in Fig. 17. The favorable comparison is proof that this method is able to reproduce existing data but it needs

to be checked against full scale data in a series of true prediction events much like SRICOS.

CONCLUSIONS

A new method called SRICOS is proposed to predict the scour depth z versus time t curve around a cylindrical bridge pier of diameter D founded in clay. The steps involved are: 1. taking samples at the bridge pier site, 2. testing them in an Erosion Function Apparatus called the EFA to obtain the scour rate $\dot{z}$ versus the hydraulic shear stress applied τ, 3. predicting the maximum shear stress τ_{max} which will be induced around the pier by the water flowing at v_o before the scour hole starts to develop, 4. using the measured $\dot{z}$ versus t curve to obtain the initial scour rate $\dot{z}_i$ corresponding to τ_{max}, 5. predicting the maximum depth of scour z_{max} for the pier, 6. using $\dot{z}_i$ and z_{max} to develop the hyperbolic function describing the scour depth z versus time t curve, and 7. reading the z vs. t curve at the time t_o to find the scour depth z_o which will develop around that pier.

A new apparatus is developed to measure the $\dot{z}$ *vs* t curve of step 2, a series of advanced numerical simulations are performed to develop an equation for the τ_{max} value of step 3, and a series of flume tests are performed to develop an equation for the z_{max} value of step 5. The method is evaluated by comparing predictions and measurements in 42 flume experiments. Future developments of SRICOS are discussed and the more general CHIMERA-RANS method is presented.

ACKNOWLEDGMENTS

This project was sponsored by the Texas Department of Transportation where Tony Schneider, Melinda Luna, and Kim Culp were enthusiastic and knowledgeable project directors. We also wish to thank Peter Smith and Jay Vose, formerly with TxDOT, for their key role in getting the project underway. At the Federal Highway Administration, Sterling Jones was very supportive and provided valuable background information. We also wish to thank Bertrand Philogene for his very useful work in reviewing the available literature,Kiseok Kwak and Seung-Woon Han for their help in data reduction.

REFERENCES

American Society for Testing and Materials, 1997, "Annual Book of ASTM Standards, Vol. 04.08: Soil and Rock," Philadelphia, Penna., USA.

Ariathurai, R., Arulanandan, K., 1978, "Erosion rates of cohesive soils," *Journal of the Hydraulics Division*, Proceedings of the ASCE, Vol. 104, No. HY2, pp. 279-283, ASCE, New York, N.Y.

Arulanandan, K., 1975, "Fundamental aspects of erosion in cohesive soils," *Journal of the Hydraulics Division*, Proceedings of the ASCE, Vol. 101, No. HY5, pp. 635-639, ASCE, New York, N.Y.

Arulanandan, K., Loganathan, P., Krone, R. B., 1975, "Pore and eroding fluid influence on surface erosion of soil," *Journal of the Geotechnical Engineering Division*, ASCE, Vol. 101, No. GT1, New York, N.Y., pp. 51-66.

Black, W., De Jongh, J. G. V., Overbeek, J. Th., Sparnaay, M. J., 1960, Transactions of the Faraday Society, London, Vol. 56, p. 1597.

Chen, H. C., Chen, M., Huang, E. T., 1996, "Chimera-RANS simulations of unsteady 3D flows

induced by ship and structure interactions," Flow Modeling and Turbulence Measurements VI, edited by C. J. Chen, C. Shih, J. Lienau, R. J. Kung, pp 373-380, A. A. Balkema Publishers, Rotterdam, Netherlands.

Chen, H. C., Patel, V. C. (1988), "Near-wall turbulence models for complex flows including separation," *AIAA Journal*, Vol. 26, No. 6, pp 641-648.

Christensen, B. A., September 1965, Discussion of the article by Partheniades, E., January 1965, Erosion and Deposition of Cohesive Soils, *Journal of Hydraulic Division*, Proceedings of the ASCE, Vol. 91, No. HY5, pp. 301-308.

Dunn, I. S., 1959, "Tractive resistance of cohesive channels, *Journal of Soil Mechanics and Foundations Division,* Vol. 85, No. SM3, Proceedings Paper No. 2062, pp. 1-24, ASCE, New York, N.Y.

Enger, P. F., Smerdon, E. T., Masch, F. D., Task Committee on Erosion of Cohesive Soils, July 1968, "Erosion of Cohesive Soils," *Journal of the Hydraulics Division*, Proceedings of the ASCE, Vol. 94, No. HY4, pp. 1017-1049.

Gudavalli, R., Ting, F., Briaud, J.-L., Chen, H. C., Perugu, S., Wei, G., 1997, "Flume tests to study scour rate of cohesive soils," Research Report to the Texas DOT, Department of Civil Engineering, Texas A&M University, College Station, Tex.

Hydrotechnical Construction, Moscow, May 1936 as quoted in Raudkivi, A. J., 1976, *Loose Boundary Hydraulics*, p. 276, Pergamon Press, New York, N.Y.

Kelly, E. K., Gularte, R. C., 1981, "Erosion resistance of cohesive soils," *Journal of the Hydraulics Division*, Proceedings of the ASCE, Vol. 107, No. HY10, pp. 1211-1224, ASCE, New York, N.Y.

Lagasse, P. F., Schall, J. D., Johnson, F., Richardson, E. V., Chang, F., 1995, "Stream stability

at highway structures," Federal Highway Administration *Report No. FHWA-IP-90-014 (HEC 20)*, Washington, D.C., pp 144.

Landers, M. N., Mueller, D. S., 1996, "Channel scour at bridges in the United States," Federal Highway Administration *Report No. FHWA-RD-95-184*, Washington, D.C., pp 140.

Laursen, E. M., 1962, "Scour at bridge crossings," Transactions of the ASCE, Vol. 127, Part 1, No. 3294, pp 166-209, ASCE, New York, N.Y.

Lyle, W. M., Smerdon, E. T., 1965, "Relation of compaction and other soil properties to erosion and resistance of soils," Trans. Am. Soc. Agric. Engrs., Vol. 8, No. 3.

Mitchell, J. K., 1993, *Fundamentals of Soil Behavior*, 2nd edition, John Wiley and Sons, Inc.,New York, N.Y., 422 pp.

Munson, B. R., Young, D. F., Okiishi, T. H., 1990, *Fundamentals of Fluid Mechanics*, John Wiley and Sons, Inc., New York, N.Y., 843 pp.

National Bridge Inventory, 1997, Bridge Management Branch, Federal Highway Administration, Washington, D.C.

Pagan-Ortiz, J. E., 1998, "Status of Scour Evaluation of Bridges Over Waterways in the United States", Proceedings of the ASCE Conference on Water Resources Engineering '98, ASCW, Reston Virginia. pp 2-4

Parola, A., 1997, "Research needs: scour at bridge foundations," *NCHRP Report*, Project 24.8, Transportation Research Board, Washington, D.C.

Perugu, S., Briaud, J.-L., Ting, F., Chen, H. C., Gudavalli, R, Wei, G., 1999, "Erosion function apparatus to study scour rate of cohesive soils," Research Report to the Texas DOT, Department of Civil Engineering, Texas A&M University, College Station, Tex.

Philogene, B., Briaud, J.-L., 1996, "Scour of cohesive soils: a literature review," Research report

to the Texas DOT, Civil Engineering, Texas A&M University, College Station, Texas.

Richardson, E. V., Davis, S. R., 1995, "Evaluating scour at bridges," Federal Highway Administration Report No. FHWA-IP-90-017 (HEC 18), Washington, D.C., pp 204.

Shaikh, A., Ruff, J. F., Abt, S. R., March 1988, Erosion rate of compacted Na - montmorillonite soils, *Journal of Geotelchnical Engineering*, ASCE, Vol. 114, No. 3, pp. 296-305, New York, NY.

Shen, H. W., Schneider, V. R., Karaki, S., 1969, "Local scour around bridge piers," Journal of the Hydraulics Division, ASCE, Vol. 95, No. HY6, pp 1919-1940, ASCE, New York, N.Y.

Shields, A., 1936, "Anwendung der Aehnlichkeits-Mechanik und der Turbulenzforschung auf die Geschiebebewegung," Preussische Versuchsanstalt für Wasserbau und Schiffbau, Berlin.

Shirole, A. M., Holt, R. C., 1991, "Planning for a comprehensive bridge safety assurance program," Transportation Research Record No. 1290, pp 137-142, Washington, D.C.

Smerdon, E. T., Beasley, R. P., 1959, "Tractive force theory applied to stability of open channels in cohesive soils," Research Bulletin No. 715, Agricultural Experiment Station, University of Missouri, Columbia, Mo.

Wei, G., Chen, H. C., Ting, F., Briaud, J.-L., Gudavalli, R., Perugu, S., 1997, "Numerical simulation to study scour rate in cohesive soils," Research Report to the Texas DOT, Department of Civil Engineering, Texas A&M University, College Station, Tex.

TABLE 1. Measured Critical Shear Stress for One Sand and One Gravel

	SAND	GRAVEL
Mean Diameter d_{50} *(mm)*	3.375	7.90
Coefficient of Uniformity C_u	1.54	1.20
Coefficient of Curvature C_c	0.835	0.969
Dry Unit Weight γ_d (kN/m^3)	13.77	11.30
Critical Shear Stress τ_c (N/m^2)	4.0	7.0
τ_c / d_{50} $(N/m^2/mm)$	1.18	0.88
Coefficient α (Eq. 7)	5.25	7.03

TABLE 2. Gravity and Van der Waals Forces for a Sand and a Clay Particle

	SAND PARTICLE	CLAY PARTICLE
Diameter d (m)	2×10^{-3}	1×10^{-6}
Weight W (N)	1.1×10^{-3}	1.36×10^{-13}
Van der Waals Attraction F_{VDW} (N)	7.85×10^{-23}	3.14×10^{-16}
F_{VDW} / W	7.1×10^{-20}	2.3×10^{-3}

TABLE 3. Measured Critical Shear Stress in Clays

AUTHORS	RANGE OF τ_c (N/m^2)
Dunn, 1959	2 - 25
Enger et al., 1968	15 - 100
Hydrotechnical Construction, Moscow, 1936	1 - 20
Lyle & Smerdon, 1965	0.35 - 2.25
Smerdon & Beasley, 1959	0.75 - 5
Arulanandan, et al., 1975	0.1 - 4
Arulanandan, 1975	0.2 - 2.7
Kelly and Gularte, 1981	0.02 - 0.4

TABLE 4. Measured Erosion Rates in Clay

AUTHORS	RESULTS	INFERRED SCOUR RATE* (mm/hr)
Richardson & Davis, 1995	Maximum Scour Depth Reached in Days	10 - 100
Arulanandan, et al., 1975	1-4 $g/cm^2/min$	300-1200
Shaikh et al., 1988	0.3-0.8 $N/m^2/min$	9-24
Ariathurai & Arulanandan, 1978	0.005-0.09 $g/cm^2/min$	1.5-27
Kelly & Gularte, 1981	0.0057-0.01 $gm/cm^2/sec$	100-180

* $Scour\ rate\ \frac{dz}{dt} = \left(weight\ loss\ rate\ per\ unit\ area\ \frac{dw}{adt} \right) \times \frac{1}{unit\ weight\ \gamma}$

TABLE 5: Properties of the Porcelain Clay

Mean Diameter d_{50} (mm)	0.0062
Sand Content (%)	0
Silt Content(%)	75
Clay Content (%)	25
Natural Water Content (%)	28.5
Plastic Limit (%)	20.2
Liquid Limit (%)	34.4
Unit Weight (kN/m^3)	18.0
Specific Gravity	2.61
Undrained Shear Strength by Mini Vane (kN/m^2)	12.5
Cation Exchange Capacity (meq/100 g)	8.3
Sodium Adsorption Ratio	5
pH	6
Electrical Conductivity (mmhos/cm)	1.2

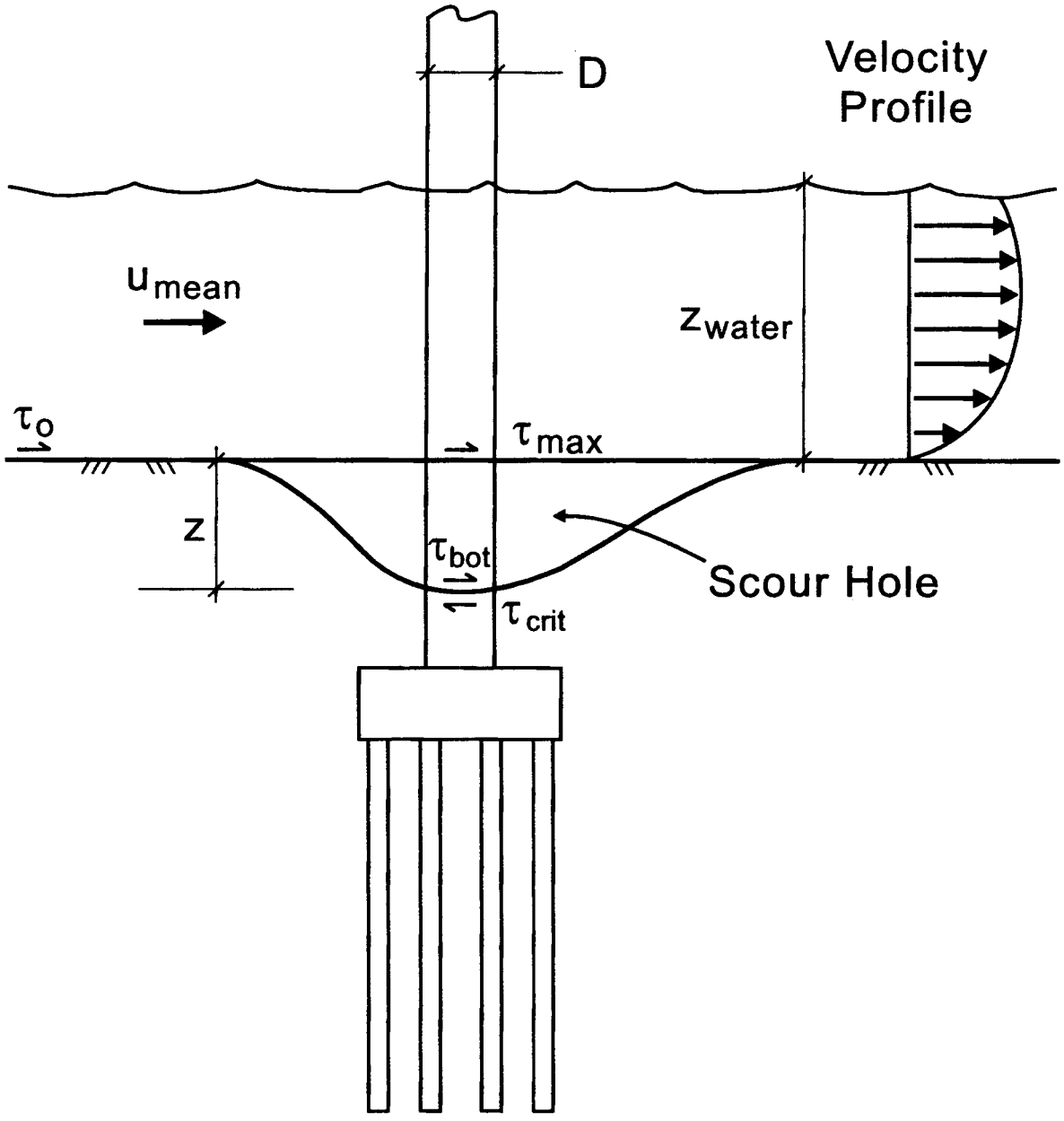

Fig. 1. Scour around a Bridge Pier

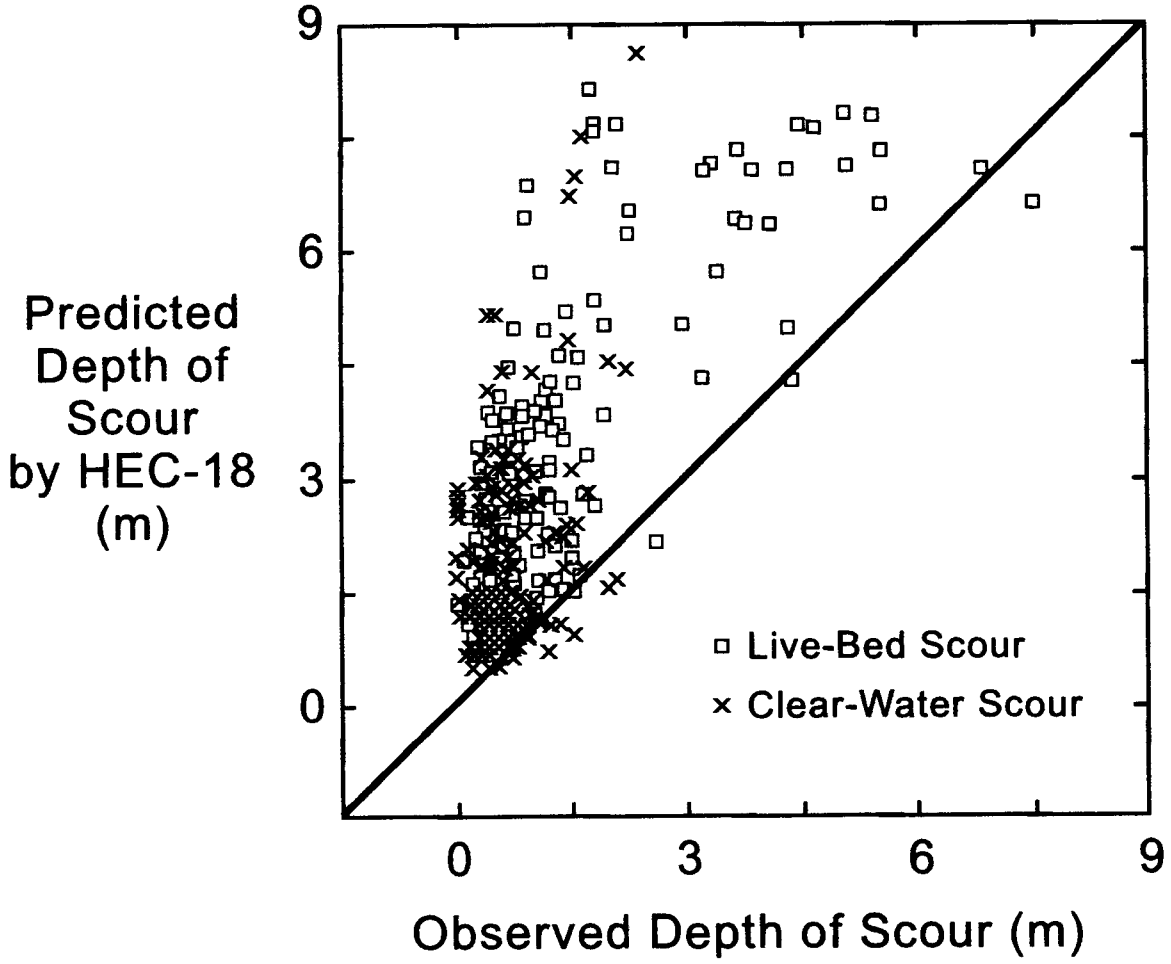

Fig. 2. Precision of the HEC-18 Equation for Maximum Depth of Scour (after Landers and Mueller, 1996)

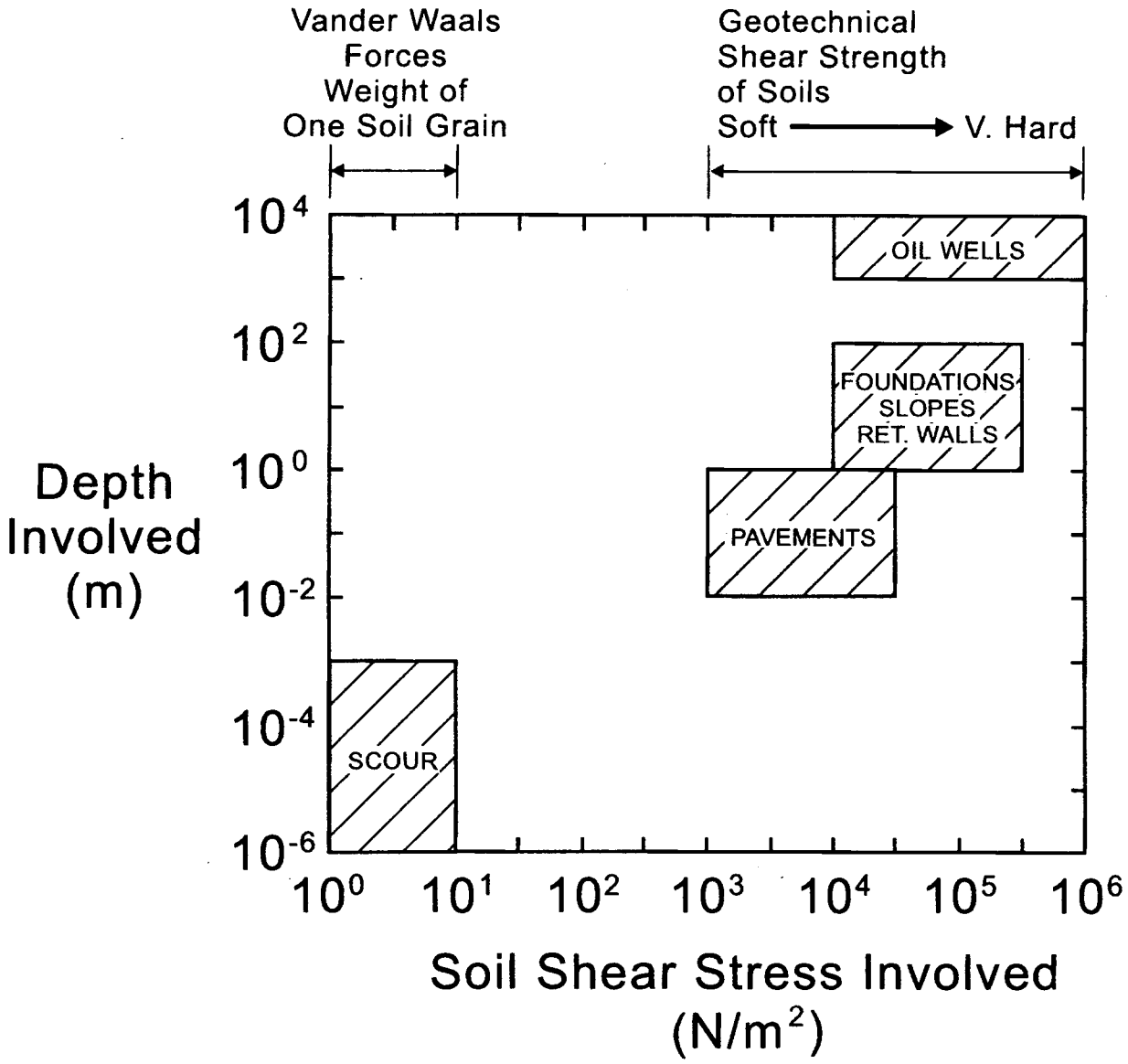

Fig. 3. Difference between Shear Stresses for Scour Problems and Foundation Problems

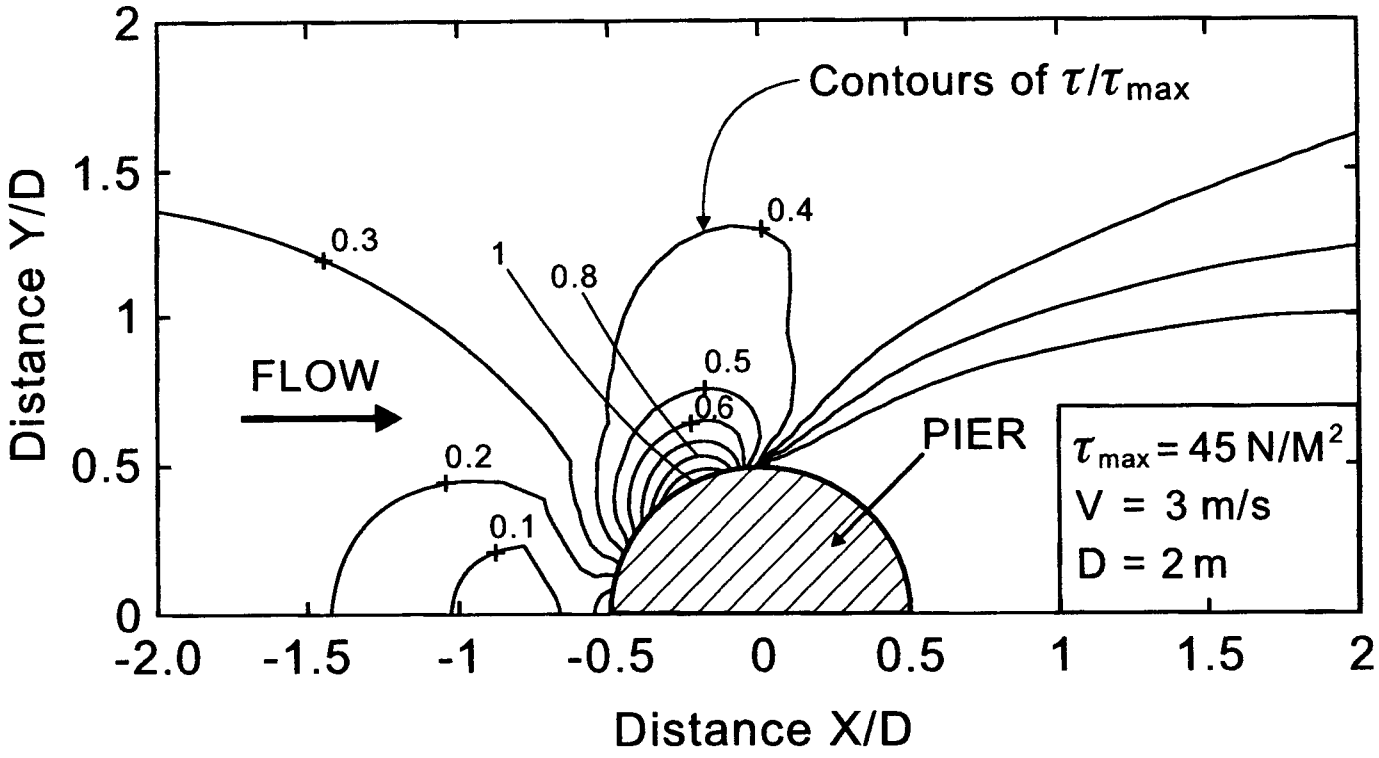

Fig. 4. Maximum Shear Stress around a Cylindrical Pier

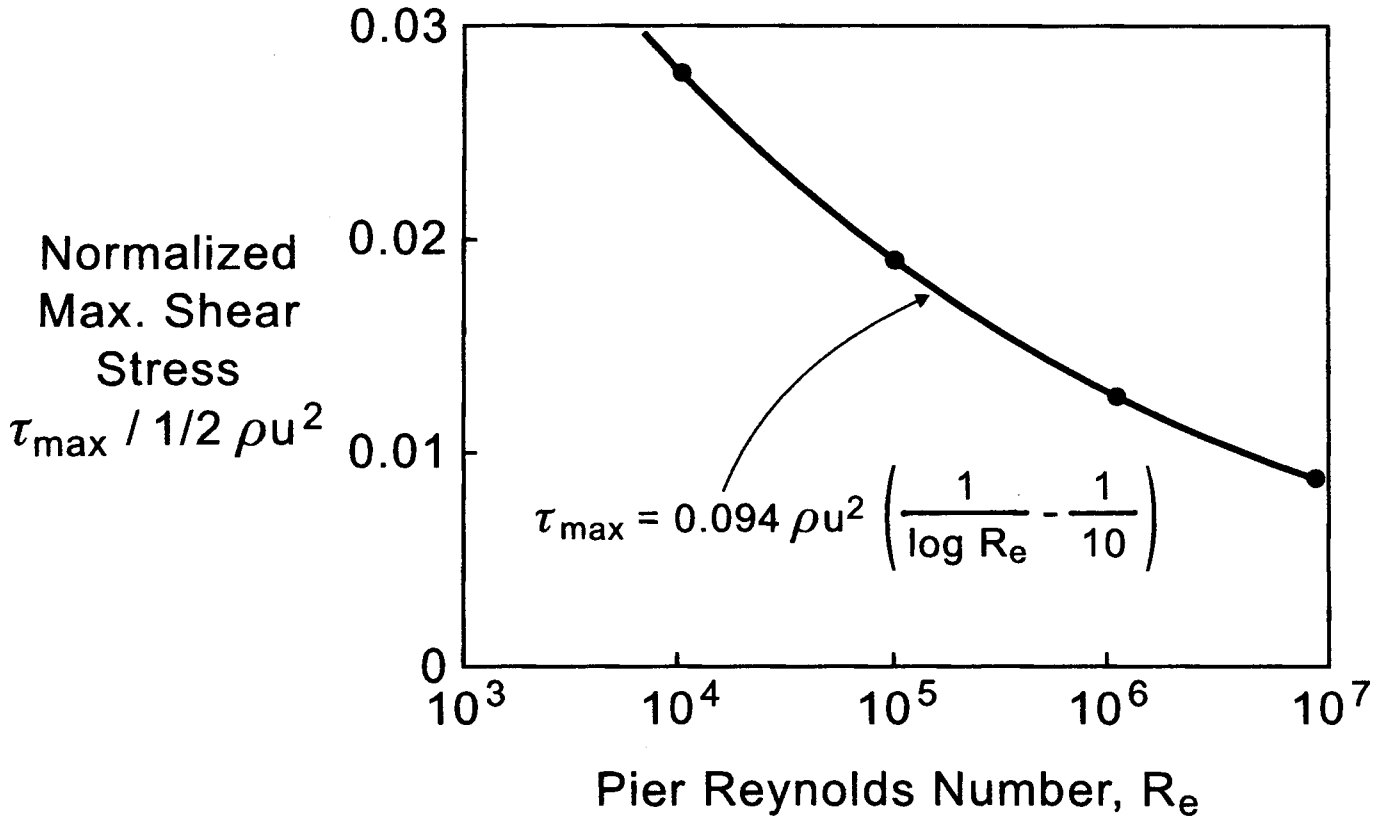

Fig. 5. Maximum Shear Stress as a Function of Reynolds Number

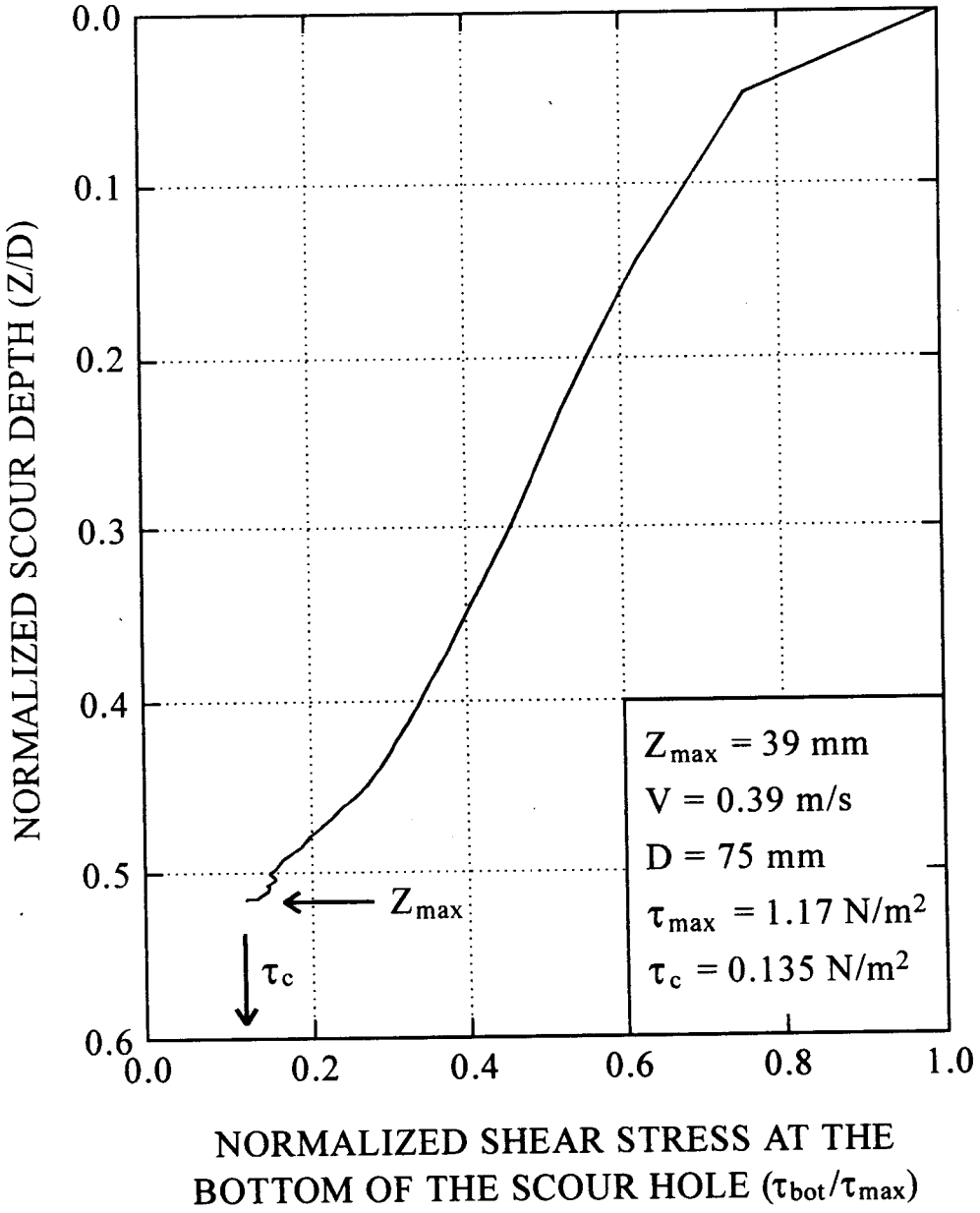

Fig. 6. Variation of the Shear Stress at the Bottom of the Scour Hole as a Function of the Depth of the Scour Hole.

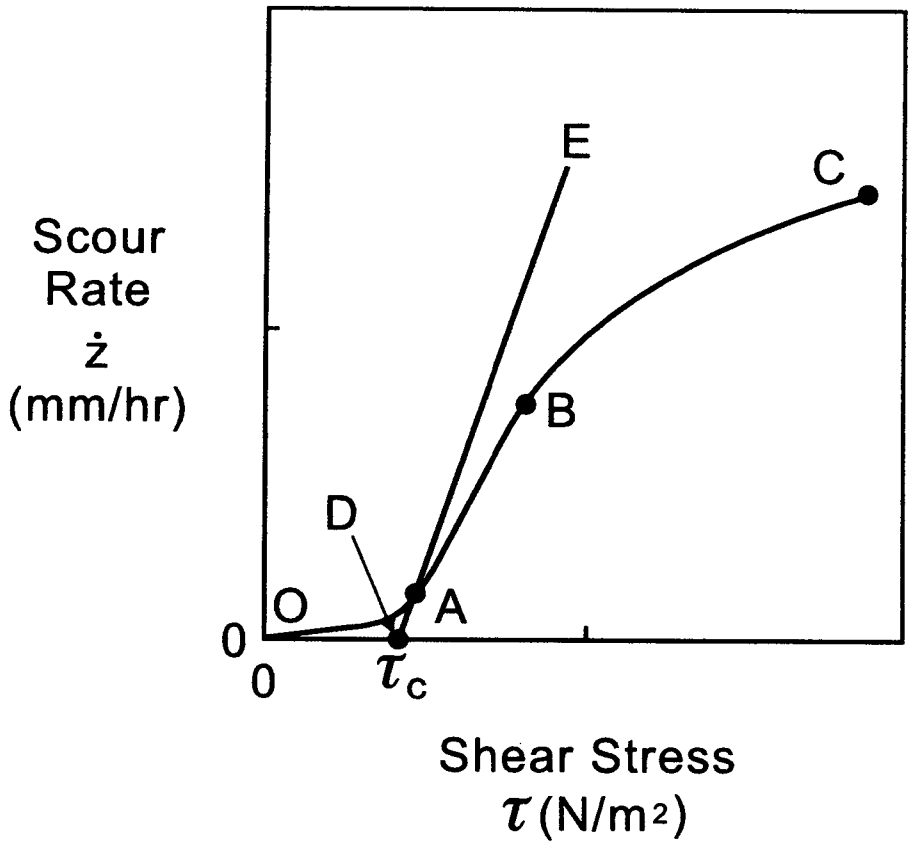

Fig. 7. Scour Rate versus Shear Stress Curve

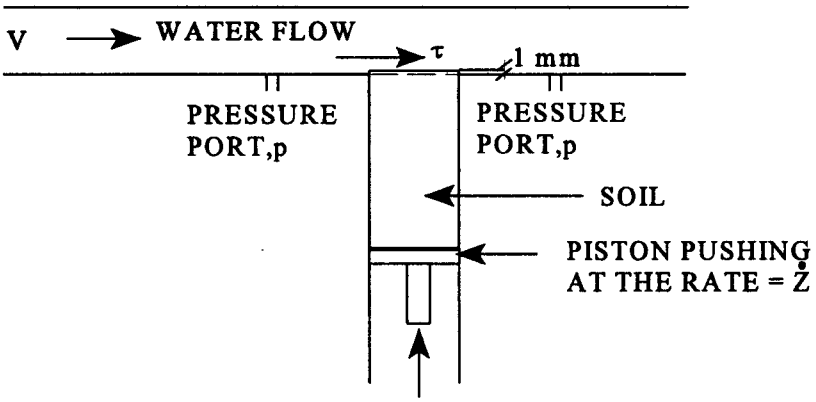

Fig. 8. The Concept of the Erosion Function Apparatus

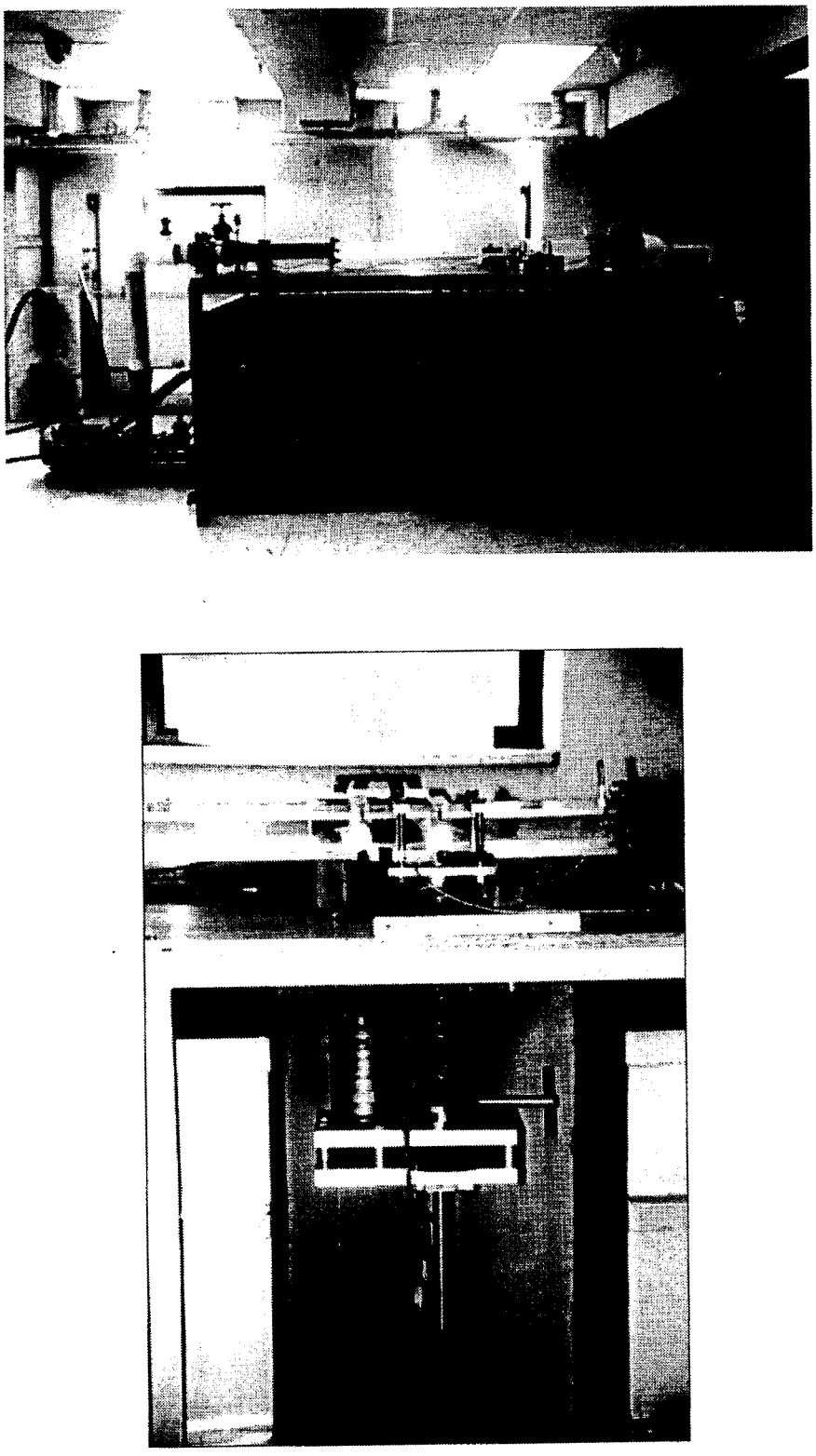

Fig. 9. The Erosion Function Apparatus

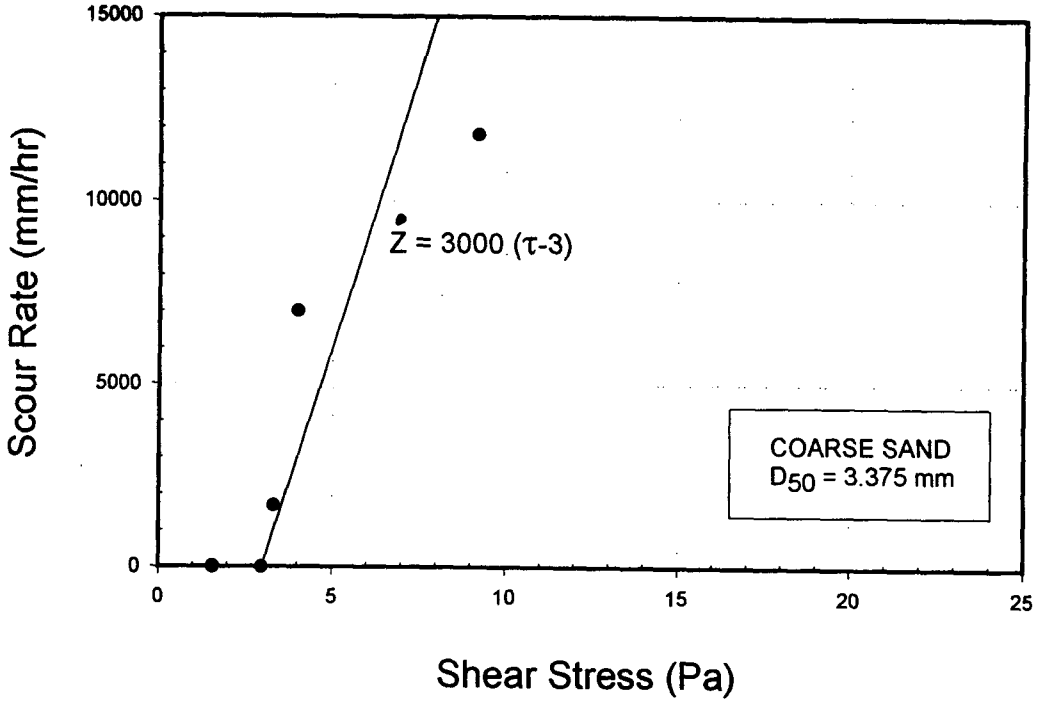

(a)

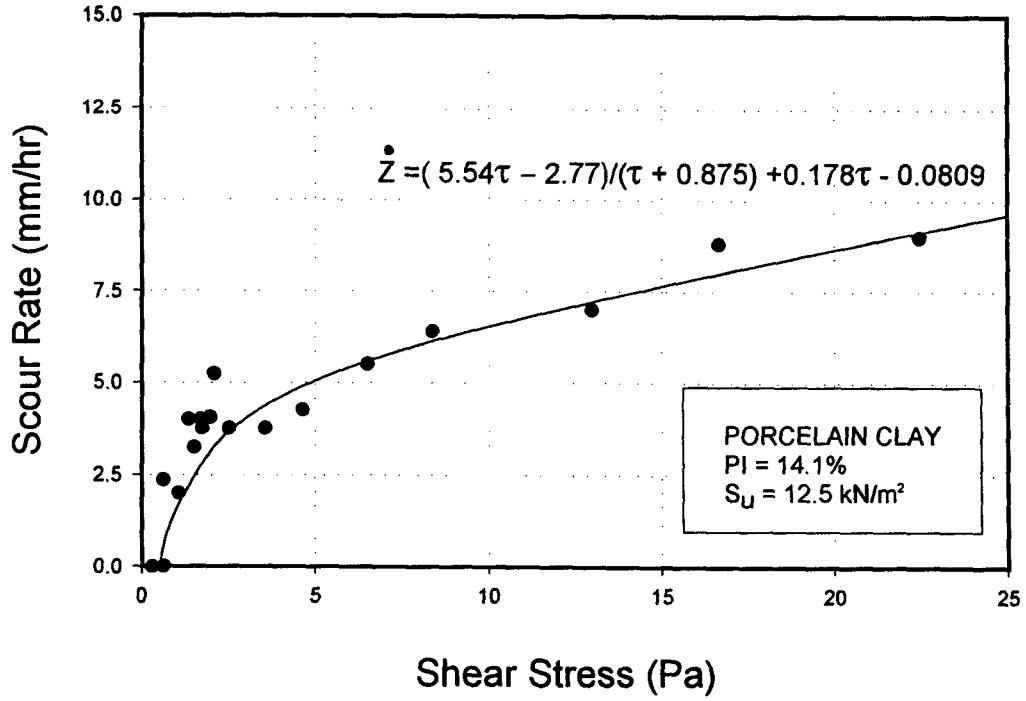

(b)

Fig. 10. Example of EFA Results (a) Sand, (b) Clay.

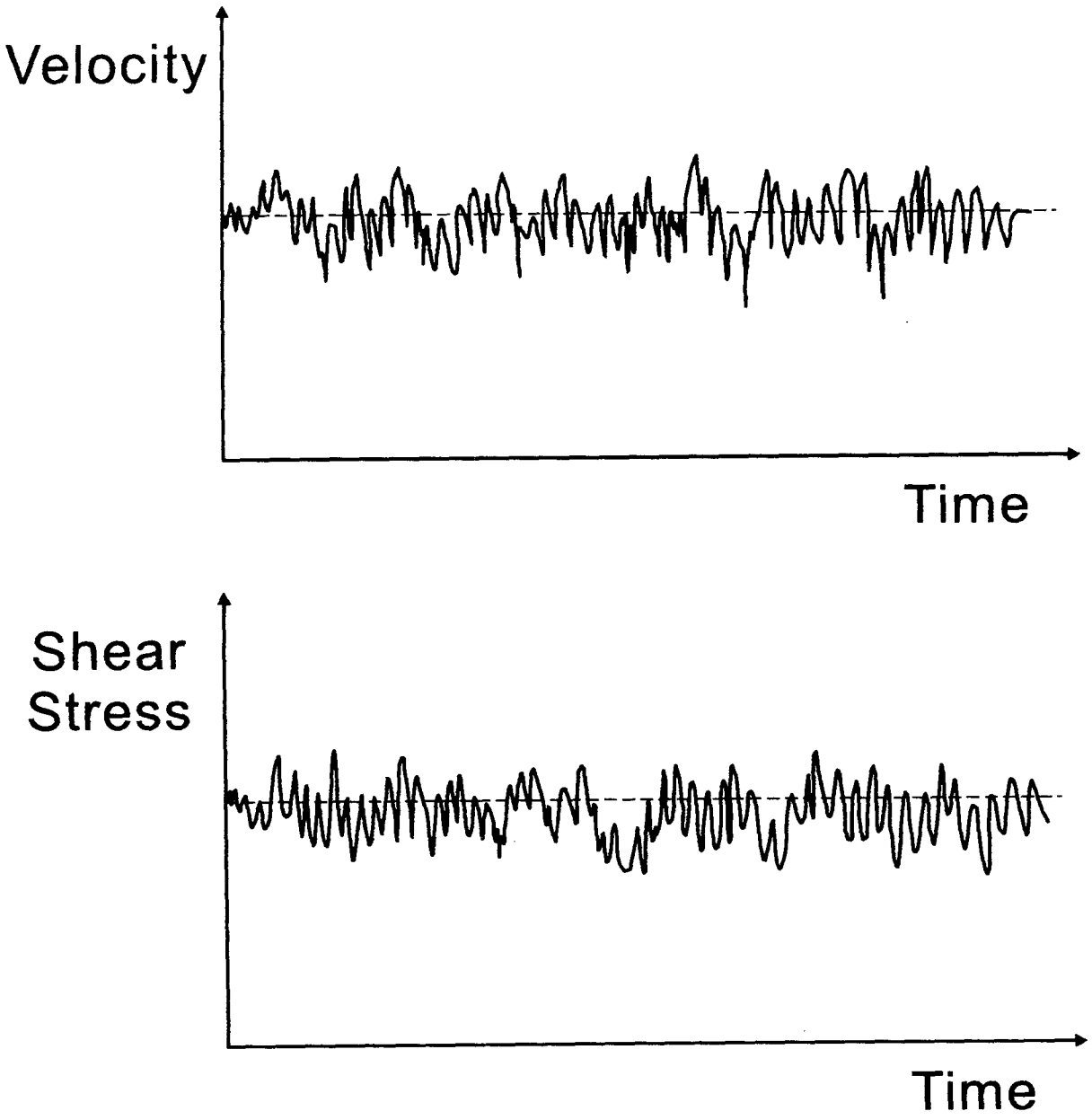

Fig. 11. Qualitative Variation of Velocity and Shear Stress in Turbulent Flow

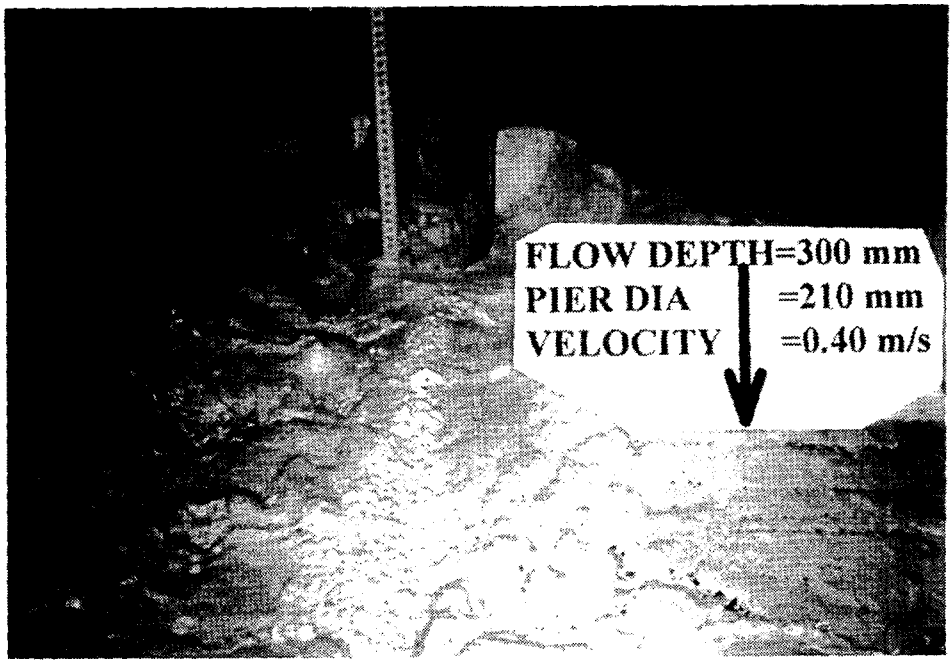

(a)

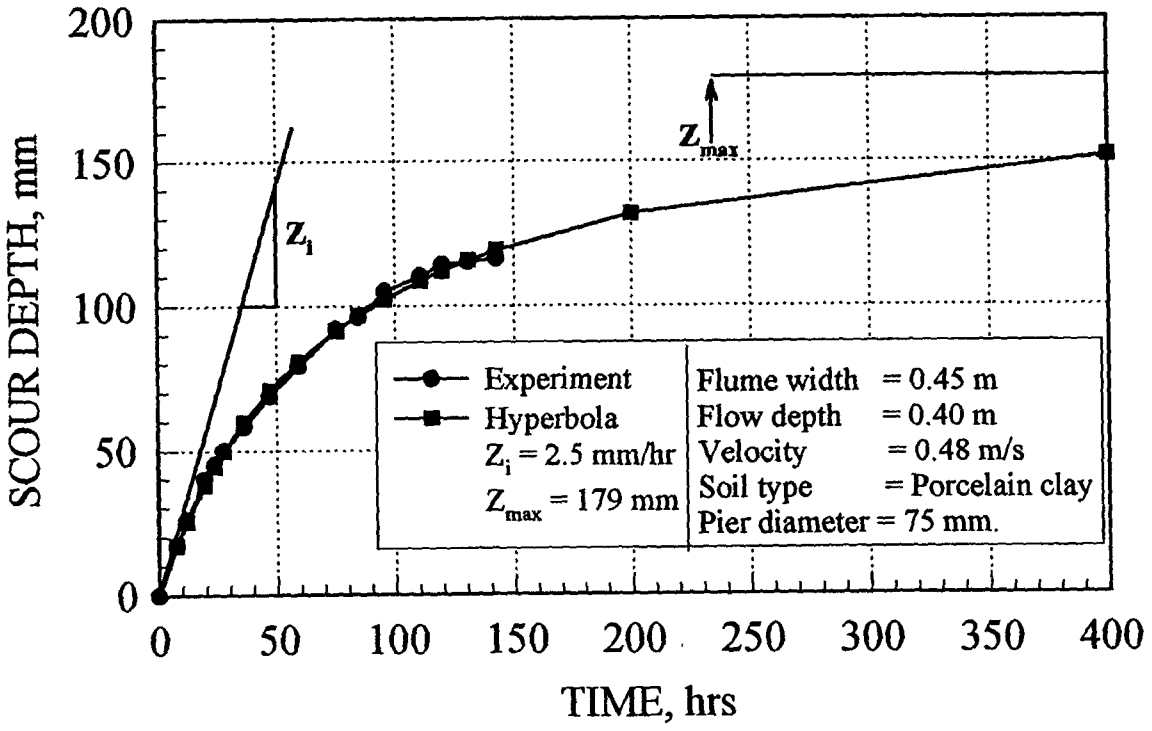

(b)

Fig. 12: Example of Flume Test Result a/ Photo of scour hole
b/ Scour Depth vs Time Curve

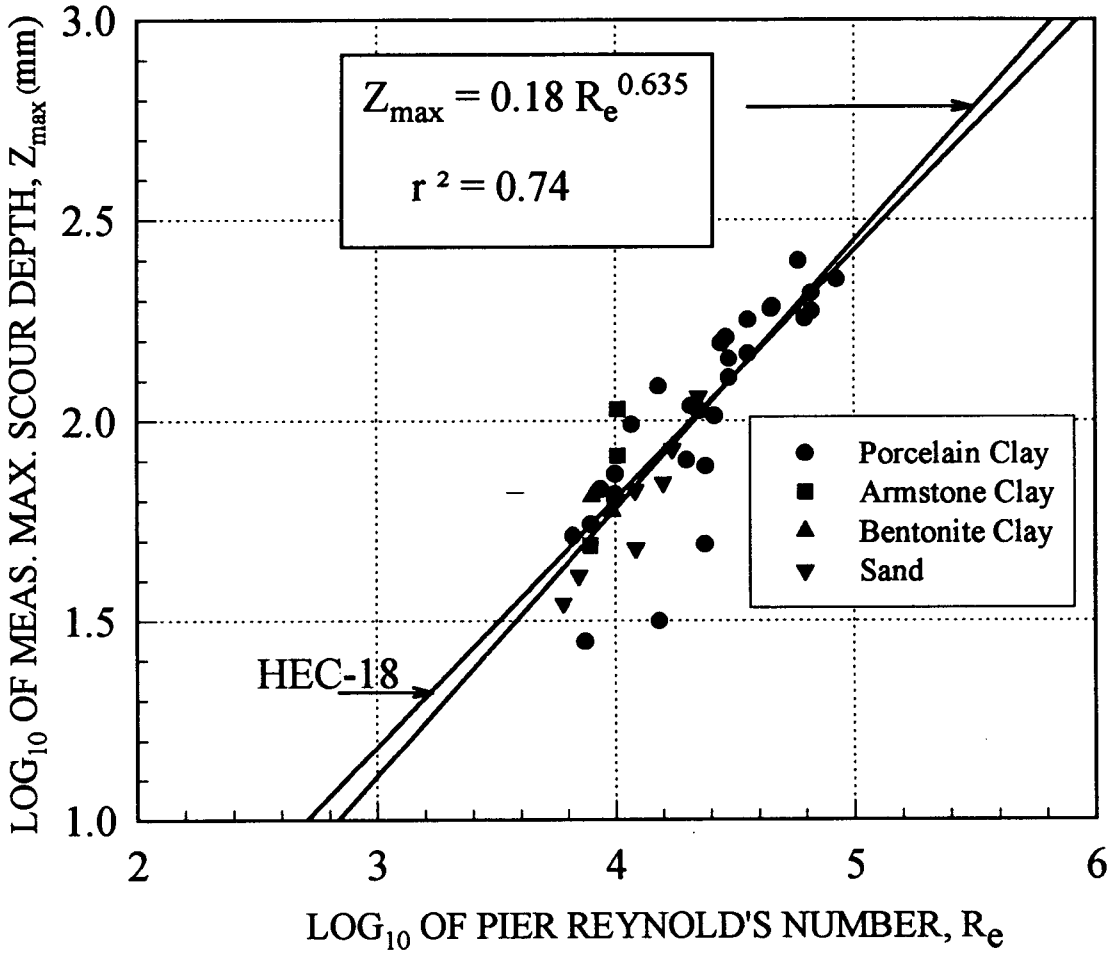

Fig. 13. Measured Maximum Depth of Scour versus Pier Reynolds Number for Flume Experiments

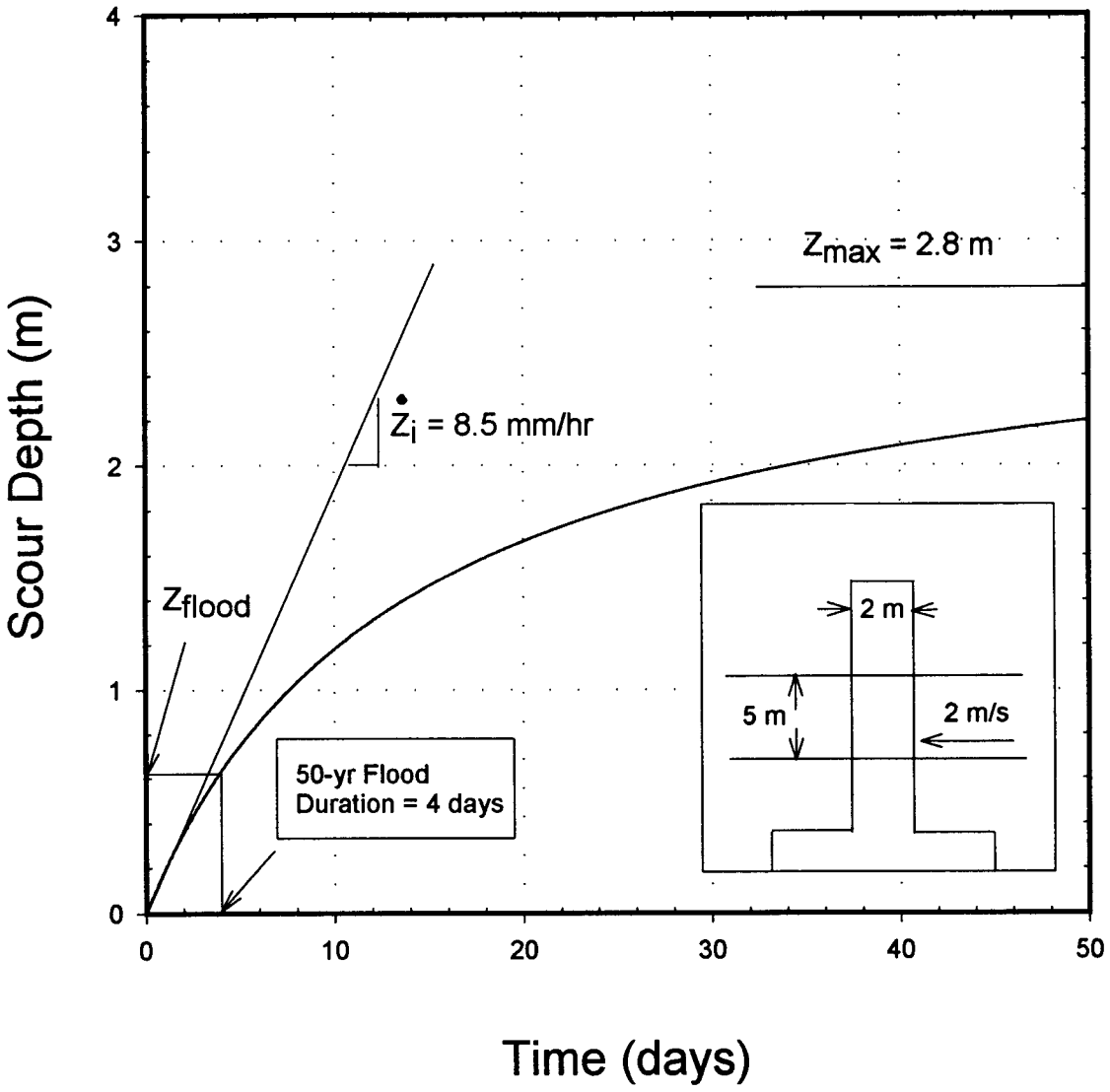

Fig. 14. Example of a Scour Depth versus Time Curve for a Full Scale Pier

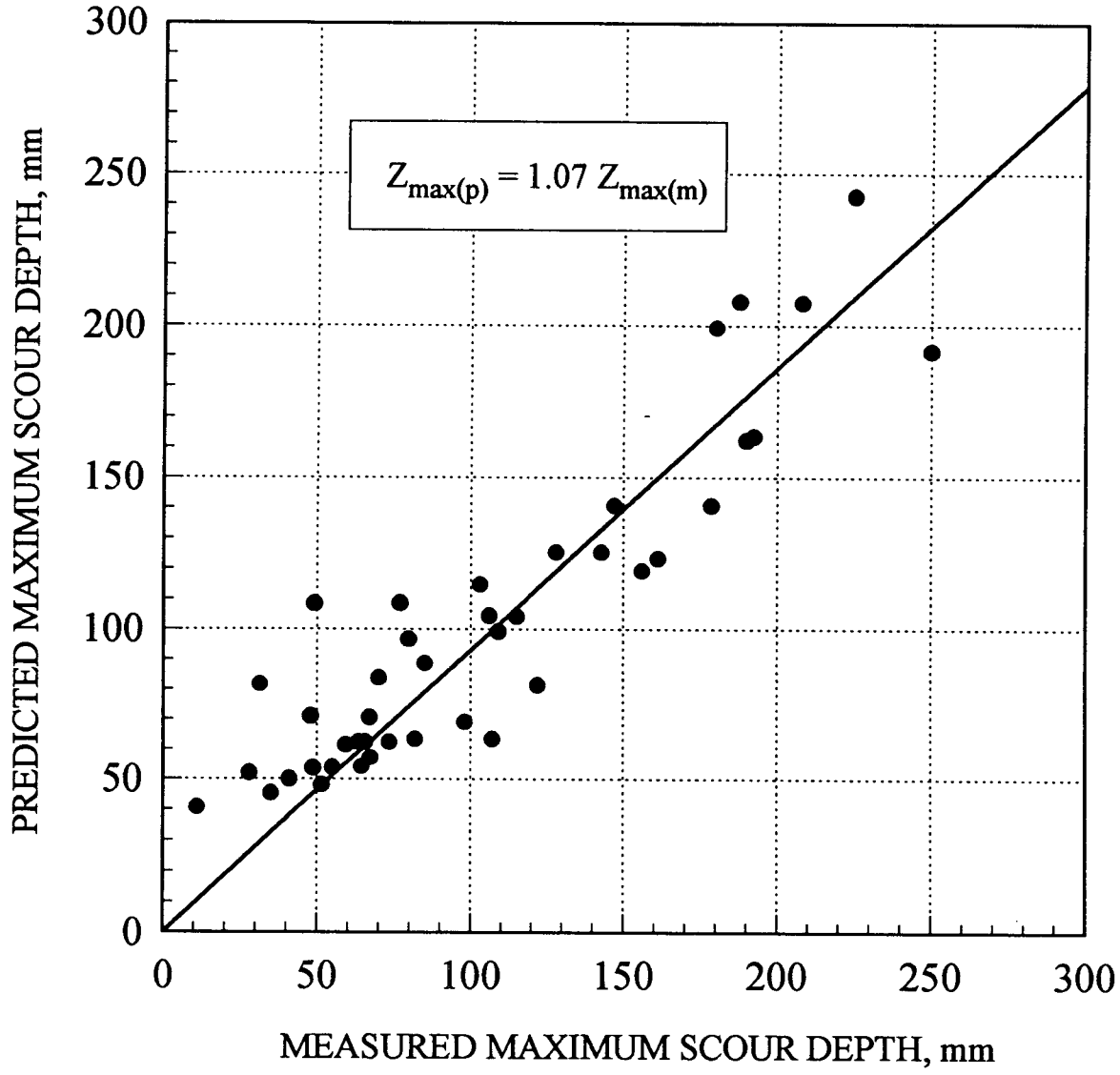

Fig. 15. Comparison of Predicted and Measured Maximum Depth of Scour

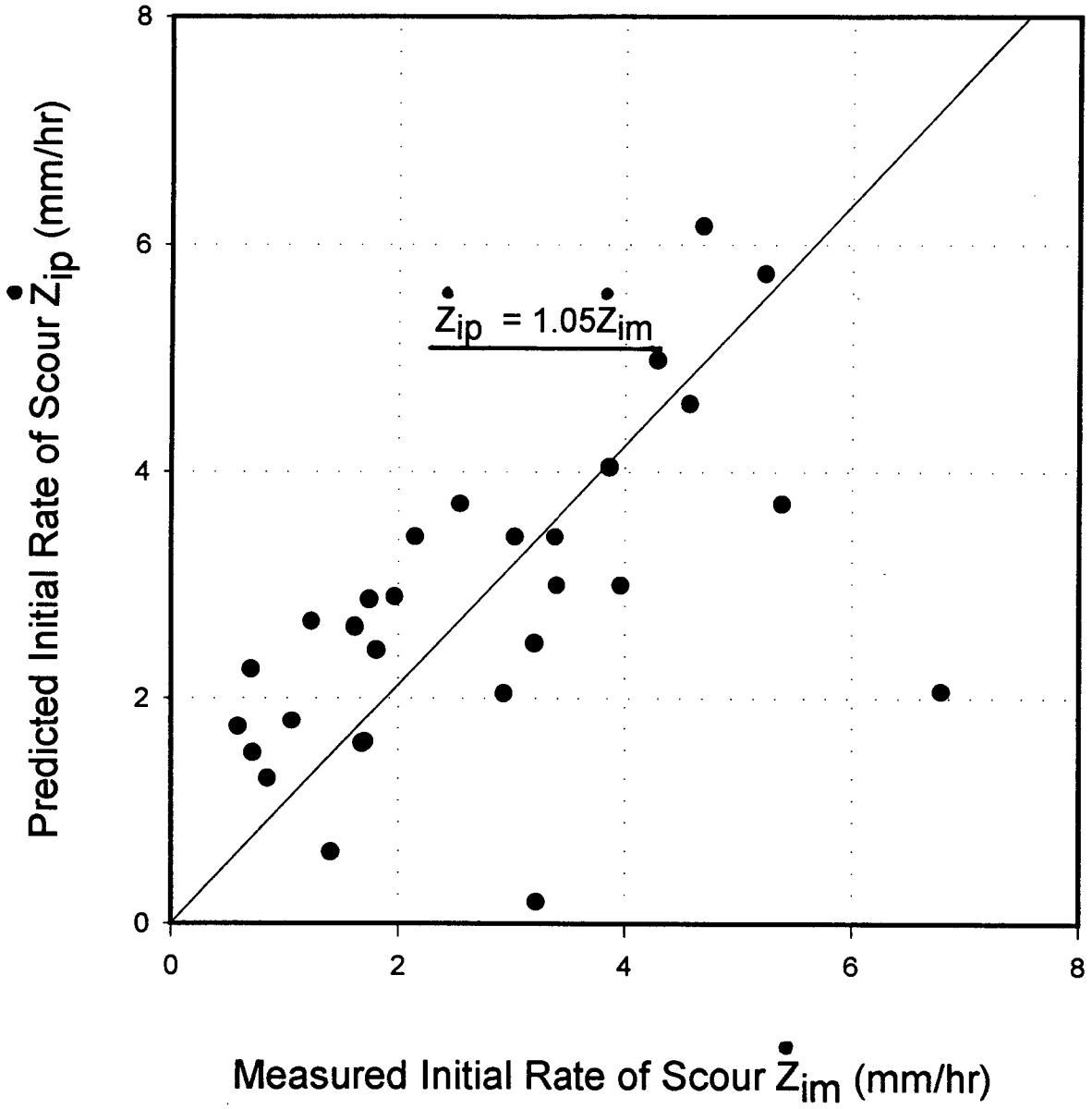

Fig. 16. Comparison of Predicted and Measured Initial Rate of Scour

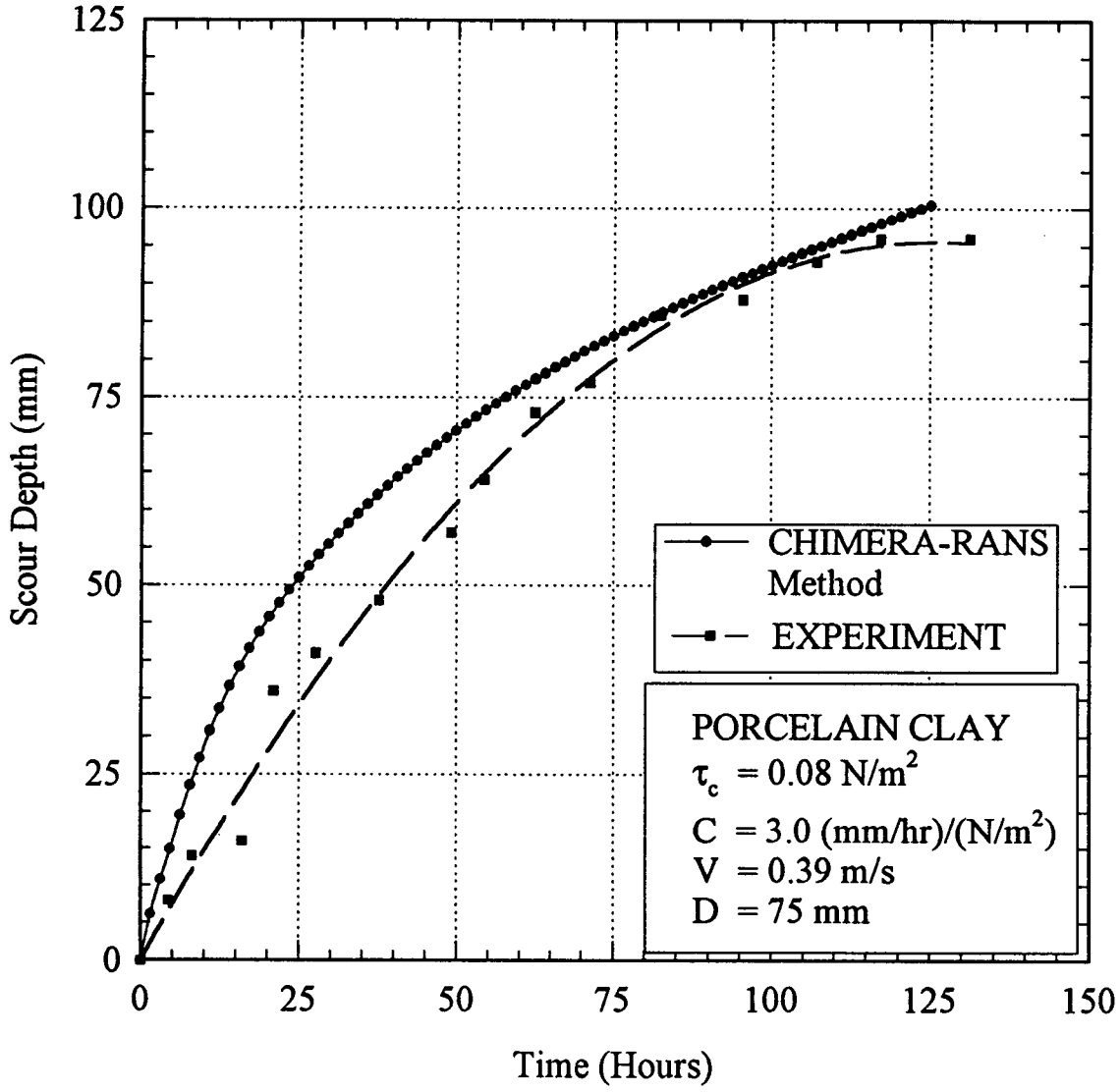

Fig. 17. Example Comparison between CHIMERA-RANS Prediction and Flume Test